An energetic stellar outburst accompanied by circumstellar light echoes

Howard E. Bond*, Arne Henden†, Zoltan G. Levay*, Nino Panagia*‡, William B. Sparks*, Sumner Starrfield§, R. Mark Wagner||, R. L. M. Corradi¶ & U. Munari#

* *Space Telescope Science Institute, 3700 San Martin Drive, Baltimore, Maryland 21218, USA*
† *Universities Space Research Association & US Naval Observatory, Flagstaff Station, PO Box 1149, Flagstaff, Arizona 86002, USA*
§ *Department of Physics & Astronomy, Arizona State University, Tempe, Arizona 85287-1504, USA*
|| *Large Binocular Telescope Observatory, University of Arizona, 933 North Cherry Avenue, Tucson, Arizona 85721, USA*
¶ *Isaac Newton Group of Telescopes, Apartado de Correos 321, 38700 Santa Cruz de La Palma, Canarias, Spain*
# *INAF-Osservatorio Astronomico di Padova, Sede di Asiago, 36012 Asiago (VI), Italy*

Some classes of stars, including novae and supernovae, undergo explosive outbursts that eject stellar material into space. In 2002, the previously unknown variable star V838 Monocerotis brightened suddenly by a factor of $\sim 10^4$. Unlike a supernova or nova, it did not explosively eject its outer layers; rather, it simply expanded to become a cool supergiant with a moderate-velocity stellar wind. Superluminal light echoes were discovered[1,2] as light from the outburst propagated into the surrounding, pre-existing circumstellar dust. Here we report high-resolution imaging and polarimetry of those light echoes, which allow us to set direct geometric distance limits to the object. At a distance of >6 kpc, V838 Mon at its maximum brightness was temporarily the brightest star in the Milky Way. The presence of the circumstellar dust implies that previous eruptions have occurred, and spectra show it to be a binary system. When combined with the high luminosity and unusual outburst behaviour, these characteristics indicate that V838 Mon represents a hitherto unknown type of stellar outburst, for which we have no completely satisfactory physical explanation.

Light echoes around a star undergoing an outburst appear after the eruption—the illumination is delayed by the longer path length from the star to the surrounding dust and then to the Earth, as compared with the light from the outburst itself travelling directly to the Earth. In the case of an instantaneous light pulse, the geometry of a light echo is straightforward[3–8]: the illuminated dust lies on the paraboloid given by $z = x^2/2ct - ct/2$, where x is the projected distance from the star in the plane of the sky, z is the distance from this plane along the line of sight towards the Earth, c is the speed of light, and t is the time since the outburst. Light echoes are rare, having been observed only around a few classical novae in our own Galaxy[3,9,10], and around several extragalactic supernovae[11]. With the exception of SN1987A (ref. 12), these echoes arose from interstellar dust or gas in the line of sight, rather than from true circumstellar material.

V838 Mon erupted in early January 2002 (ref. 13). Figure 1 shows the light curve of the outburst in linear flux units, from ground-based observations in three different wavelength bands: blue (B), visual (V) and near-infrared (I). This light curve—with a weak precursor brightening, a sharp, bright blue peak, followed by a decline and then two further broad and much redder peaks—is unlike that of a supernova, nova, or any other known type of variable star. Spectra reported by other workers (data not shown) showed a very cool photosphere throughout the outburst. Toward the end of the outburst, and during the decline, the star became extremely red. Recent spectra[14–16], taken after the decline, show that a hot B-type star is also present, along with the cool outbursting object.

We have obtained Hubble Space Telescope (HST) observations of the light echoes surrounding V838 Mon with the Advanced Camera for Surveys (ACS) at the four epochs listed in Table 1. Figure 2 shows the ACS images. Only the B filter was used at the first epoch, but for the others we obtained three-colour (BVI) frames, and have used these to make renditions that approximate true colour. The nebulosity exhibits a wealth of subarcsecond cirrus-like structure, but is dominated (especially at the first two epochs) by a remarkable series of nearly circular arcs and rings, centred on the variable star. The exact linear size of the illuminated dust envelope depends on the distance to the object, but on the basis of the distance limits given below, the visible material is confined to less than 2 pc from the star and is thus circumstellar, rather than being ambient interstellar medium. The cavity centred on the star (Fig. 2a, b), along with several features that appear aligned towards the star, also establish the circumstellar nature of the echoes.

As shown in Fig. 1, the outburst light curve had the simplest structure in the B band—a bright, relatively short peak on 6 February, and a second, weaker peak about 32 days later—making the B-band light echoes most amenable to geometric analysis. If we assume the simplest geometry, which is a series of nested spherical dust shells centred on the star and intersecting the expanding light paraboloids, then it can be shown that the apparent expansion rate of a ring is given by $dx/dt = (rc - c^2t)(2rct - c^2t^2)^{-1/2}$, where r is the radius of the ring measured from the star. Thus the time behaviour of these rings in angular units provides a direct geometric distance to the object. The pair of images taken only 20.8 days apart,

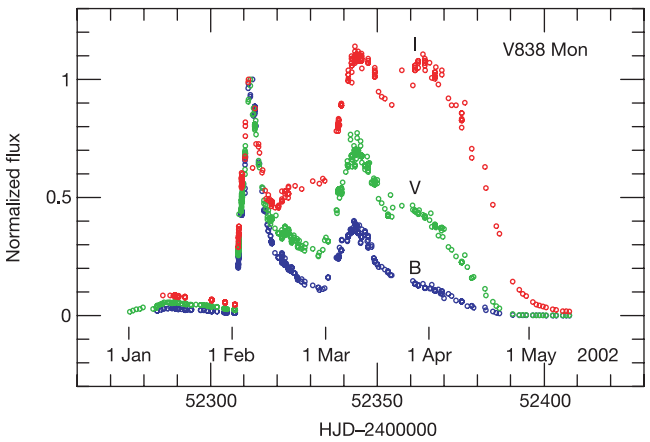

Figure 1 Multicolour light curves of the outburst of V838 Mon. Data consist of observations by A.H. (at the US Naval Observatory, Flagstaff) and by amateurs (http://vsnet.kusastro.kyoto-u.ac.jp/vsnet/index.html) and by other professional observers[2,17,26–29]. Magnitudes in the standard Johnson blue (B), visual (V), and Kron-Cousins near-infrared (I) bands have been converted to flux on a linear scale, normalized to the peak at heliocentric Julian date (HJD) 2452311. Corresponding calendar dates are shown above. After an initial rapid rise to tenth magnitude and a subsequent gradual decline, V838 Mon abruptly rose another four magnitudes in early February, reaching a maximum of $V = 6.75$ mag on 6 February 2002. After another decline, the star rose to a second peak in early March. Once again there was a slow decline after this peak, except in the I band, where yet a third peak was attained in early April. In late April, V838 Mon dropped quickly back to its original quiescent brightness in the B and V bands; this precipitous drop in brightness has been attributed to dust formation above the photosphere[29]. The progenitor object was recorded in archival sky surveys[2] at $V = 15.6$ mag, very similar to its current post-outburst brightness.

‡ On assignment from the European Space Agency, Space Telescope Division.

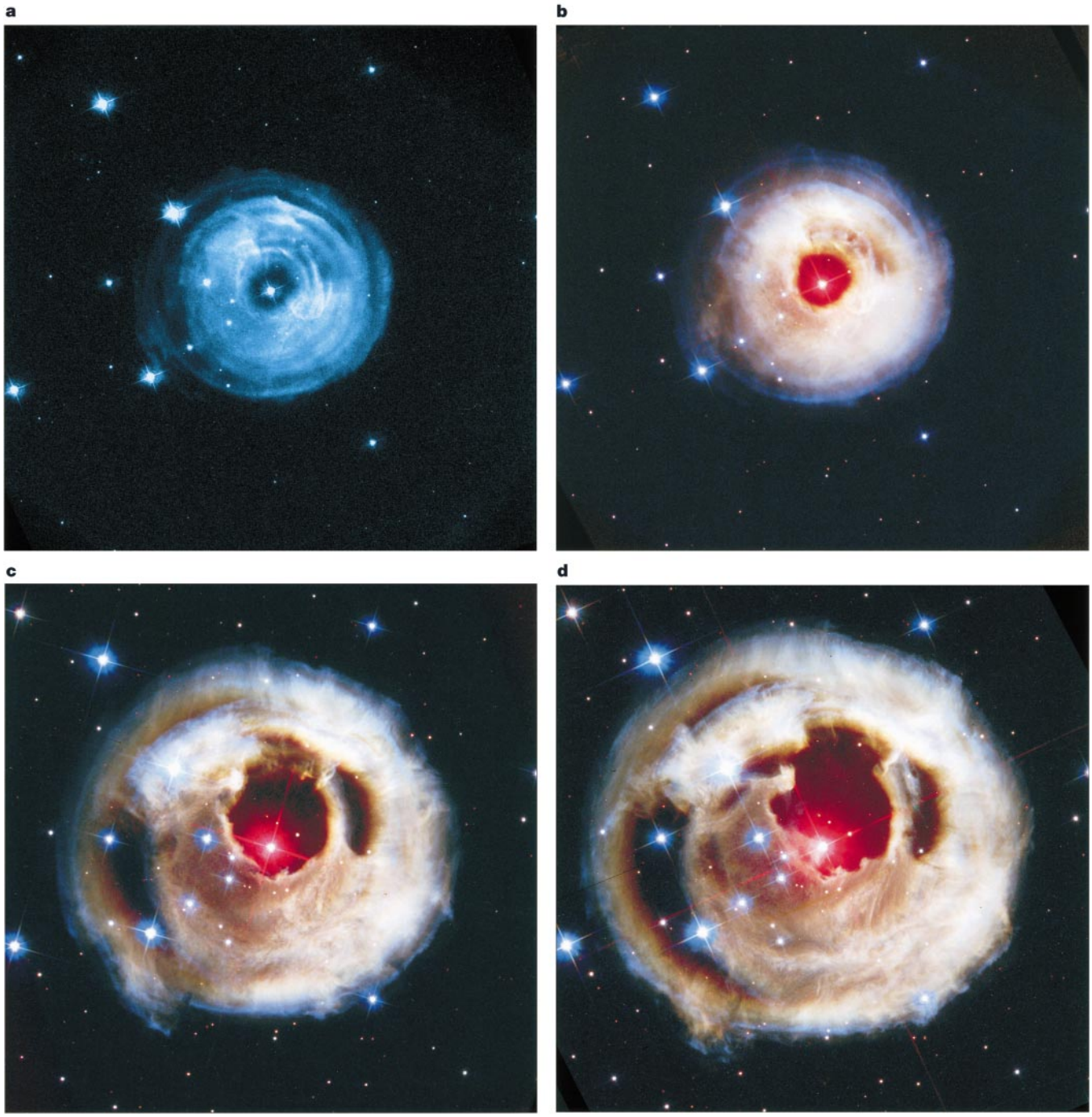

Figure 2 HST images of the light echoes. The apparently superluminal expansion of the echoes as light from the outburst propagates outward into surrounding dust is shown dramatically. Images were taken in 2002 on 30 April (**a**), 20 May (**b**), 2 September (**c**) and 28 October (**d**). Each frame is 83″ × 83″; north is up and east to the left. Imaging on 30 April was obtained only in the B filter, but B, V and I were used on the other three dates, allowing us to make full-colour renditions. The time evolution of the stellar outburst (Fig. 1) is reflected by structures visible in these colour images. In **b**, for example, note the series of rings and filamentary structures, especially in the upper right quadrant. Close examination shows that each set of rings has a sharp, blue outer edge, a dip in intensity nearer the star, and then a rebrightening to a redder plateau. Similar replicas of the outburst light curve are seen propagating outwards throughout all of the colour images.

on 30 April and 20 May, is the most suitable for such a measurement, as the same rings can be identified unambiguously in both images. The expansion rates are plotted against the mean angular radii of each ring in Fig. 3. Overlaid on the plot are the expansion rates calculated from the above equation, for ages of 62 and 93 days, which are the elapsed times between the first and second B-band light-curve peaks and the mean epoch of the two images. It can be seen that the measured points fall into two families, plotted for clarity as filled and open circles. The filled circles satisfactorily follow the expected behaviour if the corresponding echo rings are illuminated by the first light-curve peak, while the open circles appear to represent rings illuminated by the second peak. In strong confirmation of this interpretation, we find that the filled circles all refer to the blue rings seen clearly in Fig. 2b, while the open circles all correspond to the trailing, red-edged rings.

The data in Fig. 3 show significant scatter, probably arising from

Table 1 **HST observations**

UT date (2002)	HJD	Days since Feb. 6.4	Days since Mar. 10.0	ACS filters used
Apr. 30	2452394.7	82.8	51.2	B + pol
May 20	2452415.5	103.6	72.0	B + pol, V + pol, I
Sep. 2	2452520.4	208.5	176.9	B, V + pol, I
Oct. 28	2452576.0	264.1	232.5	B, V, I

The ACS filters F435W, F606W and F814W are denoted B, V and I, respectively, and '+ pol' denotes that the indicated filter was combined in succession with 0°, 60° and 120° polarizers. The time of maximum B luminosity was near 2002 February 6.4, and the second B peak was near March 10.0. (The lack of HST observations between May and September is due to solar avoidance.)

departures of the actual circumstellar structures from the simple adopted spherical geometry. For plausible non-spherical geometries, measures made over several azimuths will still average to a result close to the true distance. Thus, barring a very unusual morphology, the figure implies that the distance to V838 Mon must certainly be greater than 2 kpc, and probably significantly greater. As the predicted expansion rates approach an asymptotic limit with increasing distance, we cannot make a stronger statement at present. However, because the relations for various distances diverge with increasing time, continued high-resolution imaging will eventually yield a very precise distance.

A second, independent geometrical method for determining the distance comes from polarimetry[8]. Because maximum linear polarization occurs for 90° scattering, there will be highly polarized light at a linear radius ct, whose angular radius would thus yield the distance—but of course only if there actually is dust at that radius and at the same distance from us as the star. Our most recent polarimetric HST image, obtained on 2 September 2002, shows very high polarization (~50%), but only at the inner rim of the cavity at the lower left (southeast) of the star. Thus, at present, we can only set a lower limit to the distance, by equating the radius at this rim, ~5.0″, to ct, where t is now the time since the second light-curve peak. This lower limit is ~6 kpc. Future observations will provide a definitive distance from this method as well, once the light-echo paraboloid enlarges enough to allow illumination of close-in material behind, as well as in front of, the star. At that time, we expect to see maximum polarization in a ring[8], rather than right at the inner edge of the rim.

For a distance of at least 6 kpc (and interstellar reddening of $E(B-V) \approx 0.8$; refs 17, 18), the absolute magnitude of V838 Mon at maximum was at least $M_V = -9.6$, making it more luminous than a classical nova, and temporarily the brightest star in the Milky Way. The light curve, spectroscopic bahaviour, and high luminosity of V838 Mon are reminiscent of "M31 RV," a luminous red variable star that appeared in the Andromeda galaxy in the late 1980s (ref. 19). M31 RV reached an absolute visual magnitude at least as bright as $M_V = -9.3$ (ref. 20), but unfortunately was not well studied before it declined below detectability. V838 Mon and M31 RV (along with, possibly, the Galactic object V4332 Sagittarii; ref. 21) appear to represent a new type of outburst in which a star expands rapidly to supergiant dimensions[22], but without either the catastrophic envelope loss or the evolution to high temperature seen in classical and symbiotic novae.

In the case of V838 Mon the outburst appears to have occurred in a binary system, which may suggest an analogy with a nova system in which a thermonuclear explosion occurs on an accreting white-dwarf companion. However, a broad theoretical exploration[23] of the parameter space for thermonuclear runaways on accreting white dwarfs predicts no behaviour like that of V838 Mon. Evidently, V838 Mon has in the recent past had several similar outbursts, which produced the dust envelope that is now being illuminated. These previous outbursts appear to rule out one-time catastrophic events such as a stellar collision or merger[24], or a common-envelope interaction[25], as the energy source. Now that V838 Mon seems to be returning to its quiescent state, further observations of the system may shed light on its properties and give insight into possible outburst mechanisms for this extraordinary object. □

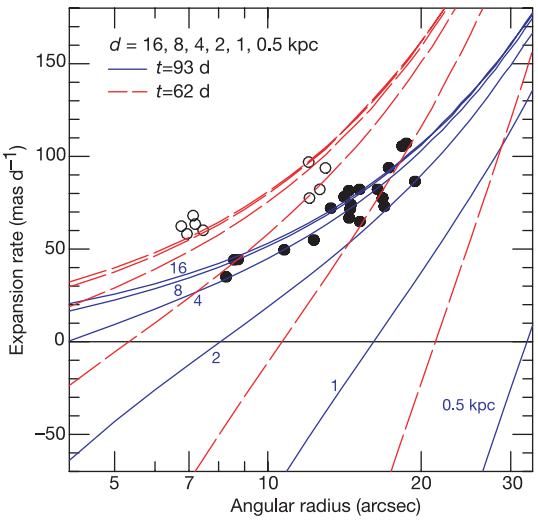

Figure 3 Measured and predicted apparent angular expansion rates of rings seen in the light echoes. Measurements were done on the pair of B-band images taken on 30 April and 20 May 2002. A simple edge-finding algorithm was used to mark the locations of the same rings on both images at several different azimuths, and their angular expansion rates were calculated. Filled circles denote rings that we attribute to illumination from the first light-curve peak, and open circles denote rings attributed to the second peak. Measurement errors are only slightly larger than the size of the plotted points. Units of expansion are milliarcseconds per day, as functions of angular radius in arcseconds. Also shown are the predicted expansion rates for light-echo rings seen 62 days (red dashed lines) and 93 days (blue solid lines) after outburst, calculated from the equation given in the text. They are functions of distance to the star, plotted for the range from 0.5 to 16 kpc, and are apparently superluminal owing to the parabolic geometry of the illuminated surfaces. The measured angular expansion rates imply a strong lower limit to the stellar distance of 2 kpc.

Received 26 November 2002; accepted 18 February 2003; doi:10.1038/nature01508.

1. Henden, A. *et al.* V838 Monocerotis. *IAU Circ.* No. 7859 (2002).
2. Munari, U. *et al.* The mysterious eruption of V838 Mon. *Astron. Astrophys.* **389,** L51–L56 (2002).
3. Schaefer, B. E. Light echoes: novae. *Astrophys. J.* **327,** 347–349 (1988).
4. Kapteyn, J. C. Über die Bewegung der Nebel in der Umgebung von Nova Persei. *Astron. Nachr.* **157,** 201–204 (1902).
5. Couderc, P. Les auréoles lumineuses des novae. *Ann. Astrophys* **2,** 271–302 (1939).
6. Russell, H. N., Dugan, R. S. & Stewart, J. Q. *Astronomy: a Revision of Young's Manual of Astronomy* 786 (Ginn, Boston, 1945).
7. Chevalier, R. A. The scattered-light echo of a supernova. *Astrophys. J.* **308,** 225–231 (1986).
8. Sparks, W. B. A direct way to measure the distances of galaxies. *Astrophys. J.* **433,** 19–28 (1994).
9. Ritchey, G. W. Nebulosity about Nova Persei. Recent photographs. *Astrophys. J.* **15,** 129–131 (1902).
10. Casalegno, R. *et al.* The emission nebula associated with V1974 Cygni: a unique object? *Astron. Astrophys.* **361,** 725–733 (2000).
11. Sparks, W. B. *et al.* Evolution of the light echo of SN 1991T. *Astrophys. J.* **523,** 585–592 (1999).
12. Bond, H. E., Gilmozzi, R., Meakes, M. G. & Panagia, N. Discovery of an inner light-echo ring around SN 1987A. *Astrophys. J.* **354,** L49–L52 (1990).
13. Brown, N. J. Peculiar variable in Monoceros. *IAU Circ.* No. 7785 (2002).
14. Geballe, T. R., Smalley, B., Evans, A. & Rushton, M. T. V838 Monocerotis. *IAU Circ.* No. 8016 (2002).
15. Munari, U. & Desidera, S. V838 Monocerotis. *IAU Circ.* No. 8005 (2002).
16. Wagner, R. M. & Starrfield, S. V838 Monocerotis. *IAU Circ.* No. 7992 (2002).
17. Kimeswenger, S., Lederle, C., Schmeja, S. & Armsdorfer, B. The peculiar variable V838 Mon. *Mon. Not. R. Astron. Soc.* **336,** L43–L47 (2002).
18. Zwitter, T. & Munari, U. V838 Monocerotis. *IAU Circ.* No. 7812 (2002).
19. Mould, J. *et al.* A nova-like red variable in M31. *Astrophys. J.* **353,** L35–L37 (1990).
20. Bryan, J. & Royer, R. E. Photometry of the unique luminous red variable in M31. *Publ. Astron. Soc. Pacif.* **104,** 179–181 (1992).
21. Martini, P. *et al.* Nova Sagittarii 1994 1 (V4332 Sagittarii): The discovery and evolution of an unusual luminous red variable star. *Astron. J.* **118,** 1034–1042 (1999).
22. Munari, U., Henden, A., Corradi, R. L. M. & Zwitter, T. in *Classical Nova Explosions* (eds Hernanz, M. & Jose, J.) 52–56 (American Institute of Physics, New York, 2002).

23. Prialnik, D. & Kovetz, A. An extended grid of multicycle nova evolution models. *Astrophys. J.* **445,** 789–810 (1995).
24. Soker, N. & Tylenda, R. Main-sequence stellar eruption model for V838 Monocerotis. *Astrophys. J.* **582,** L105–L108 (2003).
25. Iben, I. & Tutukov, A. V. Rare thermonuclear explosions in short-period cataclysmic variables, with possible application to the nova-like red variable in the Galaxy M31. *Astrophys. J.* **389,** 369–374 (1992).
26. Goranskii, V. P. *et al.* Nova Monocerotis 2002 (V838 Mon) at early outburst stages. *Astron. Lett.* **28,** 691–700 (2002).
27. Osiwala, J. P. *et al.* The double outburst of the unique object V838 Mon. in *Symbiotic Stars Probing Stellar Evolution* (eds Corradi, R. L. M., Mikolajewska, J. & Mahoney, T. J.) (ASP Conference Series, San Francisco, in the press).
28. Price, A. *et al.* Multicolor observations of V838 Mon. *IAU Inform. Bull. Var. Stars* **5315,** 1 (2002).
29. Crause, L. A. *et al.* The post-outburst photometric behaviour of V838 Mon. *Mon. Not. R. Astron. Soc.* (in the press).

Acknowledgements This Letter is based on observations with the NASA/ESA Hubble Space Telescope, obtained at the Space Telescope Science Institute, which is operated by AURA, Inc. under a NASA contract. We thank the Space Telescope Science Institute for awarding Director's Discretionary Observing Time for this project, and for support. S.S. was supported, in part, by NSF and NASA grants to Arizona State University.

Competing interests statement The authors declare that they have no competing financial interests.

Correspondence and requests for materials should be addressed to H.E.B. (e-mail: bond@stsci.edu).

Realization of the Cirac–Zoller controlled-NOT quantum gate

Ferdinand Schmidt-Kaler, Hartmut Häffner, Mark Riebe, Stephan Gulde, Gavin P. T. Lancaster, Thomas Deuschle, Christoph Becher, Christian F. Roos, Jürgen Eschner & Rainer Blatt

Institut für Experimentalphysik, Universität Innsbruck, Technikerstraße 25, A-6020 Innsbruck, Austria

Quantum computers have the potential to perform certain computational tasks more efficiently than their classical counterparts. The Cirac–Zoller proposal[1] for a scalable quantum computer is based on a string of trapped ions whose electronic states represent the quantum bits of information (or qubits). In this scheme, quantum logical gates involving any subset of ions are realized by coupling the ions through their collective quantized motion. The main experimental step towards realizing the scheme is to implement the controlled-NOT (CNOT) gate operation between two individual ions. The CNOT quantum logical gate corresponds to the XOR gate operation of classical logic that flips the state of a target bit conditioned on the state of a control bit. Here we implement a CNOT quantum gate according to the Cirac–Zoller proposal[1]. In our experiment, two $^{40}Ca^{+}$ ions are held in a linear Paul trap and are individually addressed using focused laser beams[2]; the qubits[3] are represented by superpositions of two long-lived electronic states. Our work relies on recently developed precise control of atomic phases[4] and the application of composite pulse sequences adapted from nuclear magnetic resonance techniques[5,6].

Any implementation of a quantum computer (QC) has to fulfil a number of essential criteria (summarized in ref. 7). These criteria include: a scalable physical system with well characterized qubits, the ability to initialize the state of the qubits, long relevant coherence times (much longer than the gate operation time), a qubit-specific measurement capability and a 'universal' set of quantum gates. A QC can be built using single qubit operations ('rotations') and two-qubit CNOT gates because any computation can be decomposed into a sequence of these basic gate operations[8,9]. So far, quantum algorithms have been implemented only with nuclear magnetic resonance (NMR) and ion trap systems. Recently, using NMR techniques, complex quantum algorithms such as Shor's factorizing algorithm[10] employing seven qubits have been demonstrated[11]. In NMR systems qubits are encoded in mixed states and ensemble measurements reveal the computational output. Thus, NMR implementations of a QC are not scalable in principle, although they provide an ideal system for testing procedures and algorithms.

In contrast, trapped ions allow one to prepare and manipulate pure states such that quantum computation is scalable. In addition, cooled, trapped ions exhibit unique features which make them ideally suited for implementations of a QC[12]. In particular, their quantum state of motion can be controlled to the zero point of the trapping potential[13,14], they provide a long time for manipulations of the qubits[13] encoded in long-lived internal states[3], and their quantum state can be detected with efficiencies close to 100% (ref. 15). During the past years two and four ions have been entangled[16,17], a single-ion CNOT gate[18] has been realized, and recently the Deutsch–Jozsa algorithm[19] has been implemented on a single-ion quantum processor. While the entangling operations demonstrated in ref. 17 can be used as a logic gate, a two-ion gate using individual addressing has not been demonstrated. This may serve as a key element for the further development and future perspectives towards general purpose quantum computing with trapped ions.

To implement a QC, Cirac and Zoller proposed a string of ions in a linear trap to serve as a quantum memory where the qubit information is carried by two internal states of each ion. Computational operations are carried out by addressing the ions individually with a laser beam. Single-qubit rotations are performed using coherent excitation by a single laser pulse driving transitions between the qubit states. For a two-qubit CNOT operation, Cirac and Zoller proposed to use the common vibration of an ion string to convey the information for a conditional operation (this vibrational mode is called the 'bus-mode'). This can be achieved with a sequence of three steps after the ion string has been prepared in the ground state $\langle n = 0 \rangle$ of the bus-mode. First, the quantum information of the control ion is mapped onto this vibrational mode, that is, the entire string of ions is moving and thus the target ion participates in this common motion. Second, and conditional upon the motional state, the target ion's qubit is inverted. Finally, the state of the bus-mode is mapped back onto the control ion. Mathematically, this amounts to performing the operation

Table 1 **Pulse sequence for the Cirac–Zoller CNOT quantum gate operation**

Ion 1	Ion 2	Ion 2			Ion 2	Ion 1
$R_1^+(\pi,0)$	$R_2(\pi/2,0)$	$R_2^+(\pi,0)$	$R_2^+(\pi/\sqrt{2},\pi/2)$	$R_2^+(\pi,0)$	$R_2^+(\pi/\sqrt{2},\pi/2)$	$R_2(\pi/2,\pi)$	$R_1^+(\pi,\pi)$
Mapping	Ramsey	Composite single ion phase gate				Ramsey^{-1}	Mapping^{-1}

$R_j(\theta,\varphi)$, $R_j^+(\theta,\varphi)$ denote transitions on the carrier and the blue sideband, respectively, for the jth ion. θ denotes the angle of the rotation, defined by the Rabi frequency and the pulse length; φ denotes the axis of the rotation, given by the phase between the exciting radiation and the atomic polarization.

